Growth Analysis of Hierarchical ZnO Nanorod Array with Changed Diameter from the Aspect of Supersaturation Ratio

Youguo Yan,*,† Lixia Zhou,† Zhide Han,† and Ye Zhang‡

College of Physical Science and Technology, China University of Petroleum, 257061 Dongying, Shandong, P. R. China, and Key Laboratory of Materials Physics, Anhui Key Laboratory of Nanomaterials and Nanotechnology, Institute of Solid State Physics, Chinese Academy of Sciences, P. O. Box 1129, 230031 Hefei, Anhui, P. R. China

Received: December 31, 2009; Revised Manuscript Received: January 29, 2010

One kind of hierarchical ZnO nanorod array with changed diameter was successfully synthesized using Zn powder as the source through the chemical vapor deposition method. The supersaturation ratio was considered a crucial factor determining the growth behavior of reagent species. The growth process was discussed at length, and a growth model was proposed. Another two expanded experiments were conducted to prove the validity of this growth mechanism. In addition, our proposed growth mechanism just could be used to explain some interesting experimental phenomena in preparation of ZnO nanorod arrays, viz., the obtained nanorods often had changed diameter when Zn powder was adopted as the source, and the synthesized nanorods commonly possessed correspondingly uniform diameter when ZnO and carbon powder was used as source. These growth analyses were helpful in comprehending the microcosmic growth behavior of nanostructure and provided some references in preparation of special 1-D nanostructures with definite aspect ratio. Furthermore, these obtained hierarchical nanostructures looked like potential functional blocks in nanodevices.

1. Introduction

The assemblies of low-dimensional building blocks (nanodots, nanowires, nanobelts, and nanotubes, etc.) into hierarchical architectures on various substrates have attracted great interest because of their potential applications in functional nanodevices.[1–4] As one of the most important oxide semiconductor materials, ZnO has attracted considerable attention due to its excellent optical, electrical, and piezoelectric properties and its important applications in diverse areas.[5–8] Various quasi-one-dimensional nanostructures of ZnO have been synthesized, including nanobelts,[9] nanowires,[10] nanotubes,[11] etc. Meanwhile, different self-organized hierarchical ZnO nanostructures, such as nanorings,[12] nanopropellers,[13] nanobridges,[14] nanonails,[15] nanocandles,[16] and nanocombs,[17] etc., have also been synthesized via vapor-phase processes. Among them, the nanorod/wire arrays draw more attention due to their novel applications in the nanolasings,[18] piezoelectric nanogenerators,[19] nanoresonators,[20] photonic crystals,[21] photodetectors,[22] optical modulator waveguides,[23] light-emitting diodes,[24] field emitters,[25] gas sensors,[26,27] solar cells,[28] and so on.

As far as is known, the properties of nanostructures were strongly dependent on their structures and morphologies, especially the field emission properties in ZnO nanorod arrays, which were closely related to the shape of their tips.[29,30] So, it was important to control the structure and morphology in preparation of functional nanodevices. Thus far, different ZnO nanorod/wire arrays have been successfully synthesized.[31–33] In the preparation of these ZnO nanorod arrays via the chemical vapor deposition (CVD) method, some interesting phenomena were found; viz., nanorods with changed diameter were often obtained when Zn powder was adopted as the source,[34,35] and nanorods with correspondingly uniform diameter were generally synthesized when ZnO and carbon powder was used as precursor.[36,37] Previous research paid more attention to the evolution of structure and morphology under different experimental conditions. But, research on the microcosmic growth mechanism was rarely involved. How is the hierarchical nanorod formed? Why do the reagent species have different growth behaviors under the above two conditions? These scientific questions need further in-depth study.

Herein, one kind of hierarchical ZnO nanorod array with changed diameter was synthesized adopting Zn as the source. The growth process was discussed at length, and a growth model was proposed. Also, two expanded experiments were performed to validate the growth mechanism. From the aspect of supersaturation ratio, the distinct growth behavior using different sources could be well explained. The growth mechanism analysis was helpful in understanding the relationship between the supersaturation ratio and growth behavior of hierarchical nanostructure with changed diameter, and it was valuable in realizing the controlled synthesis of complex nanostructures in the design of nanodevices.

2. Experimental Section

The typical experiment (defined as experiment I) was conducted in a conventional horizontal tube furnace. One gram of Zn powder was adopted as the source, and a cleaned Si wafer was put upon the source as a substrate to collect product. Before heating, 100 sccm high-purity argon was introduced into the reacting chamber for 30 min to purge the air, and then, 50 sccm argon mixed with 1% oxygen was introduced into the reacting chamber. The furnace was heated to 520 °C in 20 min and kept at that temperature for 30 min. After cooling, a layer of white

* To whom correspondence should be addressed. E-mail: yyg@issp.ac.cn.
† China University of Petroleum.
‡ Chinese Academy of Sciences.

10.1021/jp9122826
Published on Web 02/12/2010

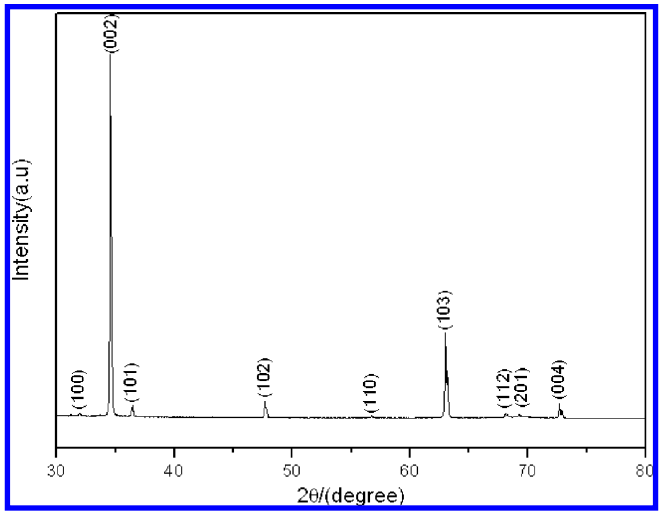

Figure 1. XRD pattern of obtained products.

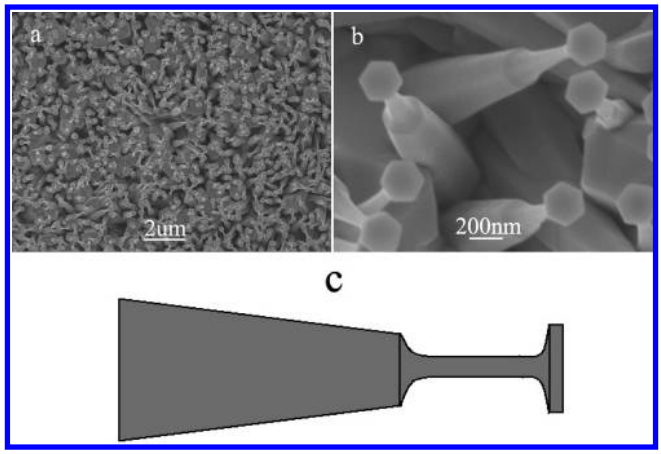

Figure 2. (a) Low- and (b) high-magnification SEM image of synthesized ZnO nanorods. (c) Configuration profile of formed ZnO nanorods: bottom nanorod with large diameter, middle nanorod with small diameter, and top hexagonal nanoplate.

products was found deposited on the substrate. Meanwhile, the surface of Zn source was found to be covered with a layer of gray hard shell, and there were some cracks on the shell. The obtained products were characterized with X-ray diffraction (XRD) spectroscopy (Philips X'pert-PRO, Cu Kα (0.154 19 nm) radiation) and field emission scanning electronic microscopy (SEM: Sirion 200 FEG).

3. Results and Discussion

3.1. Characterizations of Morphology and Structure. The X-ray diffraction pattern (Figure 1) showed that all diffraction peaks could be indexed to the hexagonal wurtzite phase of ZnO (JCPDS card: 89-0510).

The low-magnification SEM image (Figure 2a) demonstrated that bulk nanorods aligned onto the silicon substrate. The high-magnification SEM image (Figure 2b) indicated that the synthesized nanorod was composed of three sections: the bottom was nanorod with large diameter; the middle was nanorod with small diameter; the tip was hexagonal nanoplate. Figure 2c presented the profile of this hierarchical structure.

3.2. Analysis of Supersaturation Ratio. Previous research indicated that the supersaturation ratio of reagent species was an important factor affecting the growth behavior of nanomaterials.[38–41]

In our experiment, evaporated Zn vapor reacted with oxygen and formed ZnO. The reaction was the following: $Zn + O_2 \rightarrow$ ZnO. The oxygen mainly came from the carrying gas, and the supply was constant during whole reaction. The Zn vapor came from evaporation of Zn powder, and the evaporating rate was determined by several factors.

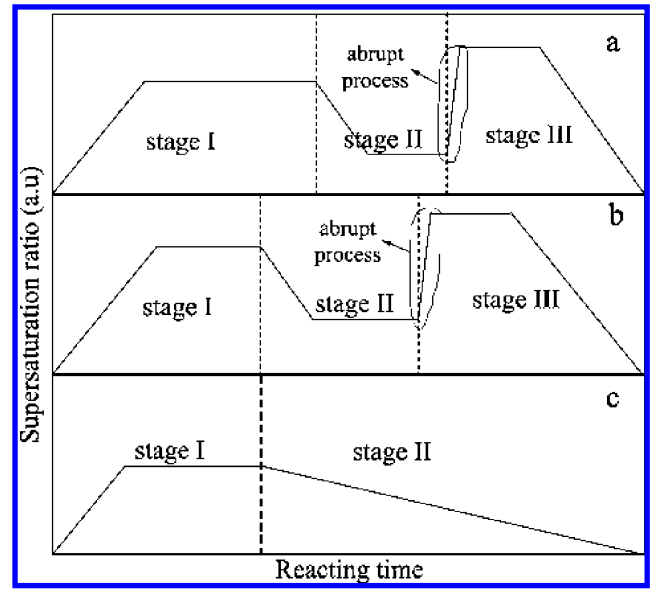

Figure 3. Changed curves of Zn supersaturation ratio during the whole reaction: curves a, b, and c represent the change of supersaturation ratio in experiments I, II, and III, respectively.

The first factor was the reacting temperature. In the heating stage, with the increase of temperature, the evaporation enhanced and the supersaturation ratio of Zn increased. When the temperature reached the settled temperature of 520 °C, the supersaturation ratio also reached maximum.

The second factor was the volatilization rate of Zn vapor from the surface of the source. In our experiment, the substrate was put upon the Zn source, so the volatilization was confined by the substrate. The evaporated Zn atoms reacted with oxygen and formed ZnO. These ZnO species would have the following behaviors: some transferred downstream with carrying flow; some deposited onto the surface of substrate to maintain the growth of ZnO nanorod; the rest dropped down to the surface of Zn source. While the reaction went along, the fallen ZnO gradually increased, and this ZnO restricted the volatilization of Zn vapor. So, in this process, the supersaturation ratio of Zn would decrease and gradually reached a minimum when the fallen ZnO formed a shell. The above conclusion just could be validated by the observed hard shell on the surface of Zn source after the reaction. Along with the heating, the evaporated Zn vapor accumulated under the ZnO shell, and the vapor pressure would gradually increase. When the vapor pressure reached a critical value, the ZnO shell would be split and this Zn vapor would be released instantly and reach the substrate. As a result, the supersaturation ratio would reach a maximum; this analysis also could be validated by the cracks found on the surface of the Zn shell.

Based on the above discussions, the supersaturation ratio of reagent species contained three stages as shown in Figure 3: initial stage with high supersaturation ratio before the ZnO shell formed; middle stage II with low supersaturation ratio after the ZnO shell formed; latter stage III with maximal supersaturation ratio after the ZnO shell was split.

3.3. Growth Mechanism. ***3.3.1. Lateral Growth and Axial Growth in the Vapor−Liquid−Solid (VLS) Mechanism.*** In the VLS mechanism, these adsorbed reagent species on the side

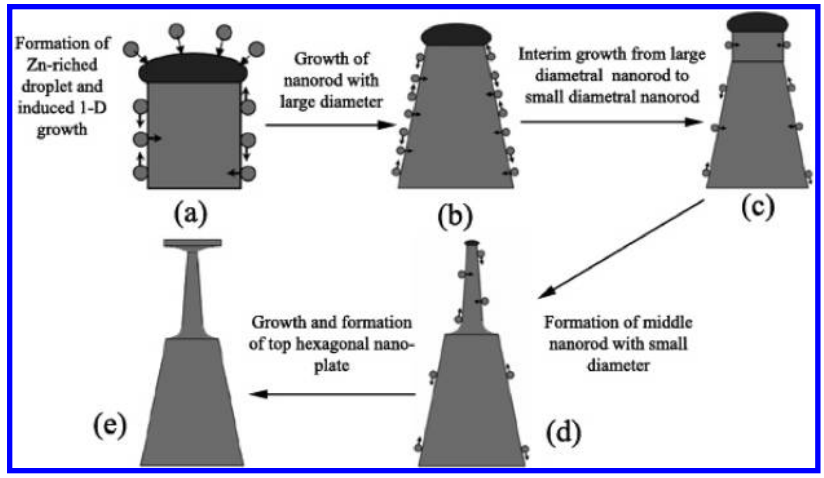

Figure 4. Growth process of ZnO nanorod corresponding to three stages of curve a in Figure 3: at stage I, formation of Zn-riched droplet and induced growth of bottom nanorod with large diameter under high supersaturation ratio; at stage II, growth of middle nanorod with small diameter under low supersaturation ratio; at stage III, growth of top hexagonal nanoplate under maximum supersaturation ratio.

surface of the formed nanorod have two growth behaviors: some transferred to the top droplet and induced axial growth; the others incorporated into the side surface of the formed nanorod and led to the lateral growth;[42,43] the diameter of the formed nanorod was determined by the ratio of lateral and axial growth rate. High ratio resulted in growth of nanorods with large diameter. In contrast, low ratio resulted in formation of nanorods with small diameter.

In the VLS growth process, the lateral growth rate was mainly determined by the mean free path which referred to the distance of two adjacent collisions of reagent species.[43] Adsorbed reagent species with large mean free path would have high probability transferring from the absorbed site to the top droplet inducing the axial growth, so the lateral growth rate was low. On the contrary, these adsorbed reagent species with small mean free path would have high probability of incorporating into the side surface to maintain a high lateral growth rate. In the growth of crystal, the mean free path was determined by the vapor pressure: the higher the vapor pressure, the smaller the mean free path. At the same temperature, the supersaturation ratio was proportional to vapor pressure. So, from the above analysis, the lateral growth rate kept a positive proportional relation with the supersaturation ratio.

The axial growth rate was determined by the definite experimental conditions. In the growth process of VLS, four consecutive steps are involved: (I) the diffusion in the vapor phase and the transference on the surface of the growing nanostructures of the reagent species; (II) the collision and injection of reagent species at the droplet surface; (III) the diffusion of the species inside the droplets; and (IV) precipitation, incorporation, and crystal growth at the liquid−solid interface between the catalyst droplet and the solid nanowire.[44] The research by Bakkers et al. indicated that step IV was the limiting step under low growth temperature,[45] and the axial growth rate was insensitive to the growing temperature. In our experiment, the reacting temperature was low (520 °C). So, the axial growth rate was low and constant during reaction.

Based on above analysis, under the experimental temperature 520 °C, the axial growth rate was constant, while the lateral growth rate was determined by the supersaturation ratio. Consequently, high supersaturation ratio would lead to growth of nanorods with large diameter. In contrast, low supersaturation ratio would result in formation of nanorods with small diameter. This point of view could be used to guide the design of special 1-D nanostructures with definite aspect ratio through modulation of the ratio of lateral and axial growth rate controlled by the supersaturation ratio.

3.3.2. Growth Model. Based on above analysis, a growth model was proposed as shown in Figure 4.

As to the growth of ZnO nanorod on Si substrate without catalyst, the nucleation could be ascribed to a self-catalyzed mechanism.[46] At the initial stage I (Figure 3) under high supersaturation ratio, a Zn-riched droplet would form and induce the 1-D growth. The formed nanorod had a large diameter due to the high lateral growth rate. The growth process was shown in Figure 4a and b. The degressive diameter from the bottom to the tip could be ascribed to the different growth time;[36] viz., the bottom formed first and had long lateral growth time, so the diameter was large. In contrast, the tip formed later and had short lateral growth time, so the diameter was small. From Figure 2b, it could be seen that the formed nanorods also have hexagonal cross section, which could be ascribed to the intrinsic hexagonal wurtzite crystallographic character of ZnO.[43] The side surface of formed nanorod was terminated with six equivalent low-index^{10,10} planes, and the surface energy was minimum.

At middle stage II (Figure 3), the supersaturation ratio was low, so the lateral growth rate decreased and formed a nanorod possessing a small diameter as shown in Figure 4c and d.

At last stage III (Figure 3), the supersaturation ratio suddenly reached a maximum. The lateral growth rate also reached a maximal value, which would result in 2-D growth, and a crystallographic symmetrical hexagonal nanoplate would form as shown in Figure 4e.

After three steps growth, a hierarchical nanorod composed of three sections with different diameters formed. The formed nanorod ended with a hexagonal nanoplate instead of a typical spherical catalyst particle in VLS growth. The disappearance of a top Zn-riched droplet could be ascribed to continuous consumption and last exhaustion during growth.[46]

3.3.3. Validity of Growth Mechanism. From the above analysis, it could be seen that our proposed growth mechanism was successful in explaining the experimental result in experiment I. But, the validity required further validation. In the growth mechanism, the supersaturation ratio was a crucial factor determining the growth behavior of reagent species. In order to prove the proposed growth mechanism, it was essential to explain other nanostructures grown with different supersaturation

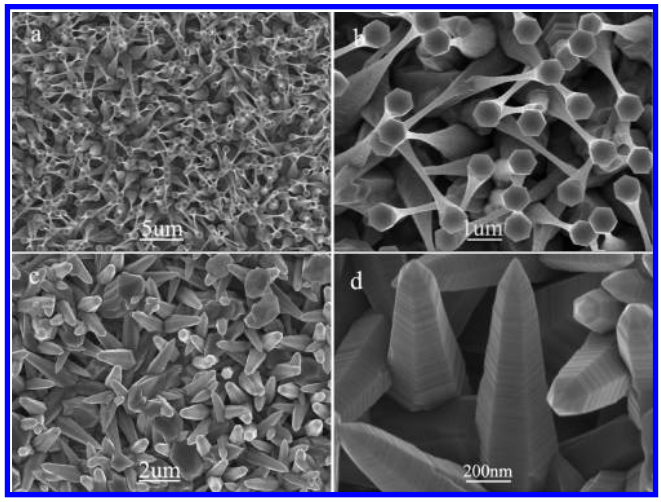

Figure 5. (a) Low- and (b) high-magnification SEM images of products with reacting temperature increased to 570 °C. (c) Low- and (b) high-magnification SEM images of products with reacting temperature decreased to 470 °C.

ratios. Therefore, another two experiments (defined as experiments II, III) were designed.

It was well-known that the supersaturation ratio of reagent species was sensitive to the temperature. In these two designed experiments, other experimental conditions were kept unchanged, and the reacting temperature was adjusted to 570 °C (experiments II) and 470 °C (experiments III), respectively.

In experiment II, after reaction, the Zn source was found to be covered by a thicker gray hard shell than that in experiment I, and there were some cracks on the shell. Based on the analysis in experiment I, the change of Zn supersaturation ratio could also be ascribed to three stages shown by curve b in Figure 3. Under high temperature (570 °C), the evaporation rate of Zn powder was accelerated and the supersaturation ratio was higher than that in experiment I. The quicker evaporation would quicken the deposition of ZnO on the surface of Zn source. So, the duration of stage I was shortened, and the formed Zn shell would be thicker. The thicker ZnO shell needs a higher critical value of vapor pressure to split it than that in experiment I. So, when the shell was split, the instantaneous release of higher-pressure Zn vapor would result in higher supersaturation ratio at stage III.

In the proposed growth mechanism, there was a crucial point; viz., high supersaturation ratio resulted in formation of nanorods with large diameter, and low supersaturation ratio resulted in formation of nanorods with small diameter. So, the formed nanorod should be composed of three sections corresponding to the three stages of supersaturation ratio. At the same time, the supersaturation ratio of curve b was higher than that of curve a at three stages. Hence, the formed nanorod should possess larger diameter than that in experiment I.

Comparing with above analysis, Figure 5a and b showed the SEM images of obtained nanorods. It could be seen that the nanorod indeed consists of three sections, the bottom was nanorod with large diameter, the middle was nanorod with small diameter, and the tip was hexagonal nanoplate. Furthermore, comparing the diameter of obtained nanorods in experiment I and II, the nanorod synthesized in experiment II possessed larger diameter than that in experiment I. The characterized results just agreed with our analysis based on our growth mechanism.

In experiment III, the temperature was decreased to 470 °C. After reaction, the Zn source was covered with a layer of gray powder, but no shell formed. Under low temperature, the evaporation of Zn powder was reduced, so the supersaturation ratio would be lower than that in experiment I. The curve c in Figure 3 showed the change of supersaturation ratio during whole reaction. Different from experiment I and II, curve C had two stages in the whole reaction; there was no abrupt change as shown in stage III in curves a and b, which originated from the split of ZnO shell in experiments I and II. At stage I, the change of Zn supersaturation ratio was the same as in experiments I and II. Due to slow evaporation of Zn vapor under low temperature, the deposited ZnO on the surface of the Zn source did not form a continuous shell after reaction. Restrained by the continuously fallen ZnO on the surface of Zn source, the evaporation rate of Zn powder gradually decreased, and the supersaturation ratio gradually decreased until the end of the reaction. From curve c, in addition to the heating stage, which might correspond to the nucleation and initial growth of the nanorod, the supersaturation ratio was monotonously degressive during the whole reaction. So, based on our growth mechanism, the diameter of formed nanorod should monotonously decrease from the bottom to the tip. Moreover, comparing experiments I and III, the lower supersaturation ratio in experiment III would result in the formation of nanorods with smaller diameter. Figure 5c and d showed the SEM images of obtained nanorods, and it could be seen that the obtained nanorods had monotonously decreased diameter and possessed smaller diameter than that in experiment I. The characterized results were also consistent with above analyses according to our growth mechanism.

These two experiments further indicated that the growth behavior of reagent species could be efficiently modulated by supersaturation ratio. The rationality of proposed growth mechanism to analyze growth behavior in these two experiments was further proved.

3.4. Explanation of Some Interesting Experimental Phenomena. Through comparison of the reported experimental results, some interesting phenomena were found. When Zn powder was adopted as the source, the obtained nanorod often possessed a changed diameter from the bottom to the tip. However, when ZnO and carbon powder was used as the source, the obtained nanorod always possessed a correspondingly uniform diameter. Why the obtained nanorods have such a huge difference in these two kinds of experiments is a question that has never been given reasonable explanation. Herein, using our proposed viewpoint, viz., diameter determined by the supersaturation, this question could be well answered.

Previous research indicated that the modes to supply reagent species for metal powder and oxide and carbon powder have large differences.[47–50] For metal powder, the supply of reagent species was through direct evaporation. The evaporating rate was sensitive to the reacting temperature, residual quantity of metal powder, and surface state, etc. So, the supply of reagent species was inconsistent with the changed experimental conditions during the whole reaction process. As to the precursor of oxide and carbon powder, the mode to supply reagent vapor was indirect carbon thermal reduction. The carbon thermal reduction was gentle and stable. So, the supersaturation ratio was correspondingly stable during the whole reaction.

Based on the proposed growth mechanism that different supersaturation ratio resulted in formation of different diameter, if Zn was adopted as the source, the fluctuant supersaturation ratio often resulted in formation of 1-D nanostructure with changed diameter. When ZnO and carbon powders were adopted as the source, the relatively stable supersaturation ratio commonly resulted in growth of nanorods with uniform diameter. In order to validate the above point, another experiment was conducted. Figure 6a and b present the SEM images of ZnO

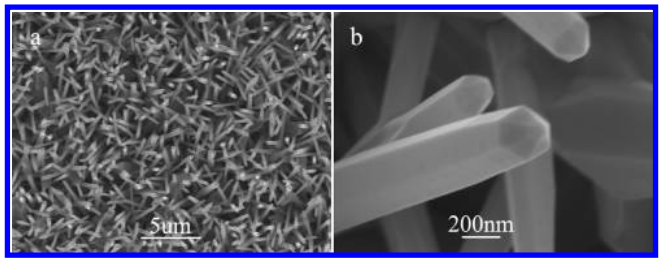

Figure 6. (a) Low- and (b) high-magnification SEM images of products with ZnO and carbon powder as source.

nanorod arrays synthesized at 1050 °C when ZnO and active carbon (with molar ratio 1:2) was adopted as the source. It could be seen that these synthesized nanorods possessed relatively uniform diameter.

From above analysis and experimental results, it could be seen that these interesting growth phenomena could be well explained by our growth model controlled by supersaturation ratio.

4. Conclusions

In conclusion, one kind of hierarchical ZnO nanorod array with changed diameter was successfully synthesized using Zn powder as the source. The supersaturation ratio was considered as a crucial factor determining the growth behavior of reagent species, and the influence of supersaturation ratio on growth behavior was discussed in detail. Based on these analyses, a growth model was proposed to explain the formation of this kind of hierarchical nanorod. The analysis indicated that high supersaturation ratio would result in formation of nanorods with large diameter. In contrast, low supersaturation ratio would result in growth of nanorods with small diameter. Another two expanded experiments were conducted to prove the validity of our growth mechanism. Some interesting experimental phenomena were also explained by our proposed model; viz., nanorods with changed diameter were often obtained when Zn powder was adopted as the source, and nanorods with correspondingly uniform diameter were generally synthesized when ZnO and carbon powder was adopted as precursor. Our analysis and discussion was helpful in understanding the microcosmic growth behavior of nanomaterial from the aspect of supersaturation ratio, and the proposed growth mechanism might have some valuable reference to guide design and synthesis of special 1-D nanostructures with definite aspect ratio. Furthermore, these obtained novel hierarchical nanostructures were also expected to have potential applications as functional blocks in future nanodevices.

Acknowledgment. This work was financially supported by the Fund for New Teachers of Education (Grant No. 20090133120004), the Basic Research Fund (Grant No. Y081817), and the School Fund (Grant No. Y081821) of China University of Petroleum.

References and Notes

(1) Ng, H. T.; Li, J.; Smith, M. K.; Nguyen, P.; Cassell, A.; Han, J.; Meyyappan, M. *Science* **2003**, *300*, 1249.
(2) Park, S.; Lim, J.-H.; Chung, S.-W.; Mirkin, C. A. *Science* **2004**, *303*, 348.
(3) Ponzoni, A.; Comini, E.; Sberveglieri, G.; Zhou, J.; Deng, S. Z.; Xu, N. S.; Ding, Y.; Wang, Z. L. *Appl. Phys. Lett.* **2006**, *88*, 203101.
(4) Hao, Y. F.; Meng, G. W.; Ye, C. H.; Zhang, L. D. *Appl. Phys. Lett.* **2005**, *87*, 033106.
(5) Fan, Z.; Lu, J. G. *J. Nanosci. Nanotechnol.* **2005**, *5*, 1561.
(6) Zeng, H. B.; Cai, W. P.; Li, Y.; Hu, J. L.; Liu, P. S. *J. Phys. Chem. B* **2005**, *109*, 18260.
(7) Zeng, H. B.; Cai, W. P.; Hu, J. L.; Duan, G. T.; Liu, P. S. *Appl. Phys. Lett.* **2006**, *88*, 171910.
(8) Zeng, H. B.; Cai, W. P.; Liu, P. S.; Xu, X. X.; Zhou, H. J.; Klingshirn, C.; Kalt, H. *ACS Nano* **2008**, *2*, 1661.
(9) Pan, Z. W.; Dai, Z. R.; Wang, Z. L. *Science* **2001**, *291*, 1947.
(10) Zheng, M. J.; Zheng, L. D.; Li, G. H.; Shen, W. Z. *Chem. Phys. Lett.* **2002**, *363*, 123.
(11) Wu, J. J.; Liu, S. C.; Wu, C. T.; Chen, K. H.; Chen, L. C. *Appl. Phys. Lett.* **2002**, *81*, 1312.
(12) Kong, X. Y.; Ding, Y.; Yang, R. S.; Wang, Z. L. *Science* **2004**, *303*, 1348.
(13) Gao, P. X.; Wang, Z. L. *J. Phys. Chem. B* **2002**, *106*, 12653.
(14) Lao, J. Y.; Huang, J. Y.; Wang, D. Z.; Ren, Z. F. *Nano Lett.* **2003**, *3*, 235.
(15) Shen, G.; Bando, Y.; Liu, B.; Golberg, D.; Lee, C.-J. *Adv. Funct. Mater.* **2006**, *16*, 410.
(16) Yan, Y. G.; Zhang, Y.; Meng, G. W.; Zhang, L. D. *J. Cryst. Growth* **2006**, *294*, 184.
(17) Wang, Z. L.; Kong, X. Y.; Zuo, J. M. *Phys. Rev. Lett.* **2003**, *91*, 185502.
(18) Huang, M. H.; Mao, S.; Feick, H.; Yan, H.; Wu, Y.; Kind, H.; Weber, E.; Russo, R.; Yang, P. *Science* **2001**, *292*, 1897.
(19) Wang, Z. L.; Song, J. H. *Science* **2006**, *312*, 242.
(20) Bai, X. D.; Wang, E. G.; Gao, P. X.; Wang, Z. L. *Nano Lett.* **2003**, *3*, 1147.
(21) Chen, Y.; Bagnall, D.; Yao, T. *Mater. Sci. Eng., B* **2000**, *75*, 190.
(22) Liang, S.; Sheng, H.; Liu, Y.; Huo, Z.; Lu, Y.; Shen, H. *J. Cryst. Growth* **2001**, *225*, 110.
(23) Lee, J. Y.; Choi, Y. S.; Kim, J. H.; Park, M. O.; Im, S. *Thin Solid Films* **2002**, *403*, 553.
(24) Saito, N.; Haneda, H.; Sekiguchi, T.; Ohashi, N.; Sakaguchi, L.; Koumoto, K. *Adv. Mater.* **2002**, *14*, 418.
(25) Li, Q. H.; Wang, Q.; Chen, Y. J.; Wang, T. H.; Jia, H. B.; Yu, D. P. *Appl. Phys. Lett.* **2004**, *85*, 636.
(26) Lin, Y.; Zhang, Z.; Tang, Z.; Yuan, F.; Li, J. *Adv. Mater. Opt. Electron.* **1999**, *9*, 205.
(27) Fan, Z.; Wang, D.; Chang, P.-C.; Tseng, W.-Y.; Lu, J. G. *Appl. Phys. Lett.* **2004**, *85*, 5923.
(28) Law, M.; Greene, L. E.; Johnson, J. C.; Saykally, R.; Yang, P. *Nat. Mater.* **2005**, *4*, 455.
(29) Zhao, Q.; Zhang, H. Z.; Zhu, Y. W.; Feng, S. Q.; Sun, X. C.; Xu, J.; Yu, D. P. *Appl. Phys. Lett.* **2005**, *86*, 203115.
(30) Kumar, R. T. R.; McGlynn, E.; McLoughlin, C.; Chakrabarti, S.; Smith, R. C.; Carey, J. D.; Mosnier, J. P.; Henry, M. O. *Nanotechnology* **2007**, *18*, 215704.
(31) Kar, S.; Pal, B. N.; Chaudhuri, S.; Chakravorty, D. *J. Phys. Chem. B* **2006**, *110*, 4605.
(32) Pan, N.; Wang, X. P.; Zhang, K.; Hu, H. L.; Xu, B.; Li, F. Q.; Hou, J. G. *Nanotechnology* **2005**, *16*, 1069.
(33) Shen, G. Z.; Bando, Y.; Chen, D.; Liu, B. D.; Zhi, C. Y.; Golberg, D. *J. Phys. Chem. B* **2006**, *110*, 3973.
(34) Han, X. H.; Wang, G. Z.; Jie, J. S.; Choy, W. C. H.; Luo, Y.; Yuk, T. I.; Hou, J. G. *J. Phys. Chem. B* **2005**, *109*, 2733.
(35) Shen, G. Z.; Bando, Y.; Liu, B. D.; Golberg, D.; Lee, C. J. *Adv. Funct. Mater.* **2006**, *16*, 410.
(36) Yuan, G. D.; Zhang, W. J.; Jie, J. S.; Fan, X.; Zapien, J. A.; Leung, Y. H.; Luo, L. B.; Wang, P. F.; Lee, C. S.; Lee, S. T. *Nano Lett.* **2008**, *8*, 2591.
(37) Wang, X. D.; Summers, C. J.; Wang, Z. L. *Nano Lett.* **2004**, *4*, 423.
(38) Ye, C. H.; Fang, X. S.; Hao, Y. F.; Teng, X. M.; Zhang, L. D. *J. Phys. Chem. B* **2005**, *109*, 19758.
(39) Leung, Y. H.; Djurisic, A. B.; Gao, J.; Xie, M. H.; Chan, W. K. *Chem. Phys. Lett.* **2004**, *385*, 155.
(40) Hao, Y. F.; Meng, G. W.; Ye, C. H.; Zhang, X. R.; Zhang, L. D. *J. Phys. Chem. B* **2005**, *109*, 11204.
(41) Hao, Y. F.; Meng, G. W.; Zhang, L. D. *Nanotechnology* **2006**, *17*, 5006.
(42) Yan, Y. G.; Zhang, Y.; Zeng, H. B.; Zhang, J. X.; Cao, X. L.; Zhang, L. D. *Nanotechnology* **2007**, *18*, 175601.
(43) Yan, Y. G.; Zhou, L. X. *Appl. Phys. A: Mater. Sci. Process.* **2008**, *92*, 401.
(44) Hao, Y. F.; Meng, G. W.; Wang, Z. L.; Ye, C. H.; Zhang, L. D. *Nano Lett.* **2006**, *6*, 1650.
(45) Bakkers, E. P. A. M.; Verheijen, M. A. *J. Am. Chem. Soc.* **2003**, *125*, 3440.
(46) Geng, C. Y.; Jiang, Y.; Yao, Y.; Meng, X. M.; Zapien, J. A.; Lee, C. S.; Lifshitz, Y.; Lee, S. T. *Adv. Funct. Mater.* **2004**, *14*, 589.
(47) Yan, Y. G.; Zhang, Y.; Zeng, H. B.; Zhang, L. D. *Cryst. Growth Des.* **2007**, *7*, 940.
(48) Yan, Y. G.; Zhou, L. X.; Zhang, Y.; Zhang, J.; Hu, S. Q. *Cryst. Growth Des.* **2008**, *8*, 3285.
(49) Yan, Y. G.; Zhou, L. X.; Zhang, Y. *J. Phys. Chem. C* **2008**, *112*, 19831.
(50) Hao, Y. F.; Meng, G. W.; Ye, C. H.; Zhang, L. D. *Cryst. Growth Des.* **2005**, *5*, 1617.

JP9122826